DESIGN AND EXPERIMENT OF GUIDANCE CAM OF AIR SUCTION GARLIC CLOVE DIRECTIONAL METERING DEVICE

/

气吸式大蒜定向排种器导向凸轮的设计与试验

Kunqiao LI, Fuhai FANG, Zhuo WANG, Yongzheng ZHANG, Mingliang ZHANG
Shandong University of Technology, College of Agricultural Engineering and Food Science, ZiBo (255000), China
Tel: +86-13015557631; E-mail: jixieshiji2021@126.com
DOI: https://doi.org/10.35633/inmateh-75-02

Keywords: *air suction type, directional metering device, guide cam, garlic, garlic clove direction*

ABSTRACT

To enhance the upright orientation rate of garlic clove bud tips, an air-suction garlic clove directional metering device with a guiding cam was developed. Key parameters influencing garlic clove discharge performance were determined through mechanical analysis. After optimization, the guiding cam's thickness (D) was set at 4 mm, with the lead-in and the seeding section tilt angles (α_t,β) of 5° and 15°, respectively. Comparative tests were conducted using optimal parameters, focusing on seed discharge disc rotational speed(n) and negative pressure (P) as main variables, with the upright rate of seeds in the receiving hopper serving as the evaluation index. Under conditions of -11.5 kPa negative pressure and 7 rad/s rotational speed, the upright rate reached 97.2%. Results demonstrated that the addition of guiding cams significantly improved the upright rate, increasing it by over 10% compared to directional metering devices without guiding cams.

摘要

为了提高排种后蒜种芽尖向上直立率低的问题。设计了一种带有导向凸轮的气吸式定向排种器，通过完成蒜种接触导向凸轮过程的力学分析，明确了影响导向排种性能的关键参数。得出导向凸轮厚度为 4mm、导入段倾斜角度为 5°、投种段倾斜角度为 15°。并且接料斗最优参数组合下进行对比验证试验，排种盘转速（n）以及负压大小(P)为试验因素，落入接料斗直立率为评价指标。增设导向凸轮排种器 p 为-11.5kPa、n 为 7rad/s 时，落入接蒜斗直立率达到 97.8%。稳定吸附时，排种器直立率之差 Δ>10%。因此，增设导向凸轮的直立率显著高于不安装导向凸轮。

INTRODUCTION

The metering device in sowing machinery typically performs four functions: seed filling, cleaning, guarding, and casting, with a guide mechanism ensuring uniform plant spacing. In garlic planting, maintaining an upright bud orientation is crucial (*Wu et al., 2024; Liu et al., 2022; Xu et al., 2021*). The garlic clove discharger must ensure uniform seed feeding in both timing and speed while discharging cloves with the bud tip upward to facilitate smooth entry into the hopper and improve seed uprightness (*Babatunde et al., 2020; Chen et al., 2016*).

Recent studies by both domestic and international scholars have led to advancements in seed guiding devices (*Kang et al., 2022; Zhao et al., 2018; Liao et al., 2020; Liu et al., 2015)*. A belt-type, high-speed corn seed guiding device using a rotating clamping method to improve seed entry accuracy and stability was developed (*Ma et al., 2023)*. A soybean precision seeding device was designed to ensure consistent grain spacing (*Chen et al., 2022)*. A corn posture-controlled seeding device that optimizes the seed guiding trajectory to maintain constant seed placement and speed was introduced (*Dong et al., 2023)*. A finger-driven, synchronous belt seed guiding system was developed (*Liu et al., 2017)*. John Deere of the United States created a brush belt seed guiding device to ensure stable seed guidance at high speeds (*Ji et al., 2021)*. The seeds discharged from the seed meter are thrown onto the partition of the conveyor belt by turning the fingers. The seeds move to the seeding port along the conveyor belt and are delivered to the seed furrow at a consistent speed (*Liu et al., 2020)*.

The primary goal of seed guidance design is stable, accurate seeding. While prior research focuses on non-directional crops, this study introduces a fixed guide cam for air-suction garlic seeders, ensuring cloves discharge with the bud tip upward for smooth hopper entry.

MATERIALS AND METHODS

Principle and composition of the guided cam working profile

The air-suction garlic seeding device rotates at speed n, guiding suction holes through seed suction (*I*), directional (*II*), and discharge (*III*) areas, as shown in Figure 1. In the suction area, cloves are captured; in the directional area, they align tangentially with the suction hole's center circle, maintaining an attitude angle of −15° to 15°. In the discharge area, cloves are released with the bud tip upward. Positioning the discharge point at *S* (horizontal) causes instability due to height, while lowering it to P resolves this. The guide cam adjusts the deflection angle for proper orientation, making its contour and position critical.

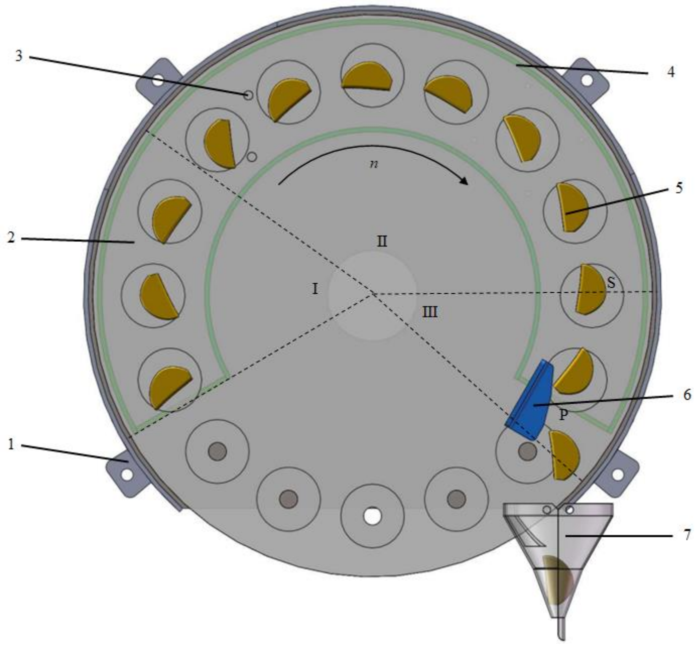

Fig. 1 - Working principle diagram of a seed tray

1 - Shell; 2 - Seed plate; 3 - Directional needles; 4 - Negative pressure chamber; 5 - Garlic clove; 6 - Guide cam; 7 - Hopper.

The guide cam's working profile comprises two curved sections, *ab* and *bc*, connected smoothly by rounded corners. In-plane projection, these sections appear as straight lines. When garlic cloves contact the *ab* and *bc* sections, their posture and deflection angles are adjusted, correcting the 30° deflection at point *P* observed without a guide cam. This ensures the cloves fall smoothly into the receiving bucket with the bud tip facing upward, completing the guiding and seeding process.

Guided Process Analysis

The guiding process of garlic cloves was analyzed using a plane analytical method to examine the contact torque between cloves and the guide cam. Contact types include side edge and arc surface contact. For side edge contact, the cloves' posture angle at point *S* ranges from -15° to 15°, with contact occurring along varying straight-line segments. A coordinate system *X* and *Y* with point *b* as the origin was established to analyze the garlic clove contact, as shown in Fig.2.

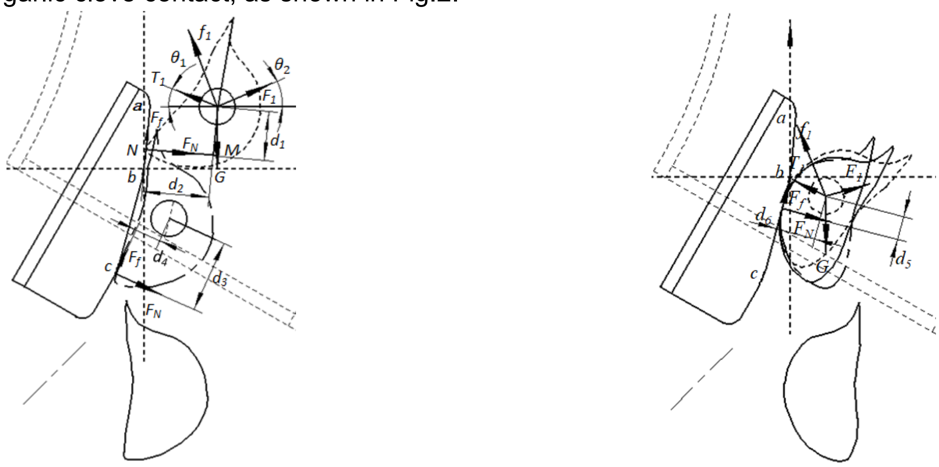

a) Garlic clove side edge contact *b) Arc contact*

Fig. 2 - Analysis of garlic clove contact guide cam process

When the garlic clove first contacts the *ab* segment, as shown in Fig.2 (a), the counterclockwise torque (M_1) must exceed the clockwise torque (M_2) to meet the guidance requirements, as shown in formula (1).

$$\begin{cases} M_1 > M_2 \\ M_1 = F_N \cdot d_1 \\ M_2 = F_f \cdot d_2 \end{cases} \tag{1}$$

where: M- rotational torque of garlic clove, N·mm;

d - rotational force arm of garlic clove, mm;

F_N, F_f- the force of the guide cam relative to the garlic clove, N;

The force arm (d) is defined as the distance from the center of the suction hole to the straight line (l). The expression for the force arm is determined by solving the equations of the two straight lines.

$$\begin{cases} y_1 = \dfrac{1}{\tan a_t} \cdot x_1 \\ y_2 = -\tan a_t x_2 + \dfrac{\sqrt{x_a^2 + y_a^2}}{\cos a_t} \end{cases} \tag{2}$$

Garlic clove rotation arm(d) is obtained, as shown in formula (3):

$$d_1 = \frac{\left| \tan a_t x_b + y_b - \dfrac{\sqrt{x_a^2 + y_a^2}}{\cos a_t} \right|}{\sqrt{1 + \tan^2 a_t},}, \quad d_2 = \frac{\left| -\dfrac{1}{\tan a_t} x_b + y_b \right|}{\sqrt{-\dfrac{1}{\tan^2 a_t} + 1}} \tag{3}$$

where: y_1, y_2 - expression for straight line segment l_{MN}, l_{ab};

α_t- the lead-in section (ab) tilt angle, °;

Taking the suction hole as the origin, F_N and F_f are obtained by analyzing the force on the garlic clove.

$$\begin{cases} T_1 \cos\theta_1 = F_1 \cos\theta_2 \\ F_f = \mu F_N \\ F = \sqrt{F_N^2 + F_f^2 + 2F_N F_f \cos\theta_3} \end{cases} \tag{4}$$

where: θ_1 - angle between centripetal force (T) and horizontal direction, °;

θ_2 - angle between resultant force (F_1) and horizontal direction, °;

θ_3 - the angle between the force (F_N) and the friction force (F_f), °;

T - centripetal force on a garlic clove, *N*;

Substituting Formula (4), and Formula (3) into Formula (1), Formula (5) can be obtained by simplifying it:

$$\left(\sin a_t + y_b \cos a_t - \sqrt{x_a^2 + y_a^2} \right) \cdot F_N > \; x_b \cos a_t + y_b \sin a_t \;\; \cdot F_f \tag{5}$$

The analysis of formula (5) reveals that counterclockwise rotation requires a relationship between αt and contact point positions (x_a, y_a). When the garlic clove first contacts the *bc* segment (Figure 2b), and the adjustment angle *β* aligns with the clove's deflection angle, the force arm $d_3 > d_4$, making *β* crucial for guiding. Therefore, the parameters α_t, *β*, and the contour require precise design.

Determination of guide cam profile

The guide cam's position and contour were optimized using Jinshan garlic as the study object. Most cloves, measuring 27-34 mm in length and 16-23 mm in width, account for 96% of the total sample, with larger cloves contacting the guide cam earlier. For analysis, a clove length of 34 mm and width of 20 mm were selected. Initial contact scenarios were evaluated to determine the guide cam's position parameters.

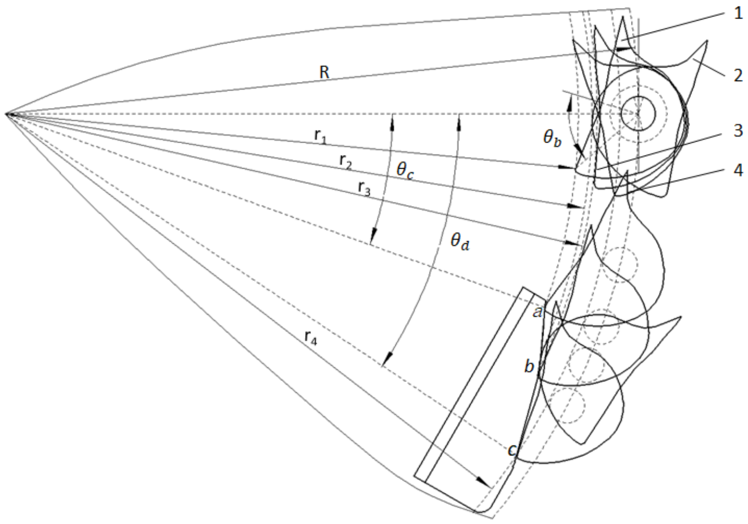

Fig. 3 - Schematic diagram of the position where the garlic clove first contacts the guide cam
1 - Side edge contact θ_z =15°; 2 - Arc contact θ_z =15°; 3 - Side edge contact θ_z =0°; 4 - Side edge contact θ_z =-15°.

The design conditions for guide cam points a, b, and c are as follows: First, when θ_z is 15°, the side edge contacts point *a* at a distance r_1 from the center, ensuring that cloves of various sizes make contact with the ab segment. Second, when θ_z is 15°, the arc surface contacts point b at a distance r_2 from the center, positioning the force below the suction hole. At θ_z, the side edge passes smoothly through point b, and at θ_z is -15°, it contacts point *c* at a distance r_4 from the center, as shown in figure 3. This design ensures garlic cloves maintain contact with the guide cam before separating from negative pressure, optimizing the guidance effect.

$$\begin{cases} \tan\theta_b = \dfrac{L/2}{D/2} \\ r_1 = R - \dfrac{D}{2\cos\theta_b}\cdot\cos\left(90^\circ - \theta_b\right) \\ r_2 = R - \dfrac{D}{2\cos\theta_b} \\ r_3 = R - \dfrac{D}{2} \\ r_4 = R - \dfrac{D}{2\cos\theta_b}\cos\left(\theta_b + 15^\circ\right) \end{cases} \tag{6}$$

where: R - Radius from the center of the suction hole to the center of the seed plate, mm;
θ_b -The angle between the length L and width B of the garlic clove,°.

The dimension parameters of the guide cam *ab* segment meet the following requirements:

$$129.47\text{mm} \approx r_1 < 134.2\text{mm} \approx r_2 < r_3 < r_4 \approx 141.35\text{mm} \tag{7}$$

From formula (7), point a is positioned at r_1 = 130mm, point b at r_2 = 135mm, and point c at r_4 = 140mm.

Determination of guide cam thickness and installation position

The precise guiding of garlic cloves depends on the thickness of the guide cam and its distance from the seed plate. An improper distance can lead to ineffective contact or tipping of the garlic clove. Measurements of Jinxiang garlic cloves indicate side edge contact points (l_1) ranging from 2.6mm - 4.8mm and arc surface contact points (l_2) from 5.1mm - 7.2mm. Consequently, the distance between the guide cam's center line and the seed plate (T) was set at T=5mm. The final thickness was established at D=4mm, ensuring effective guidance for 98% of the cloves.

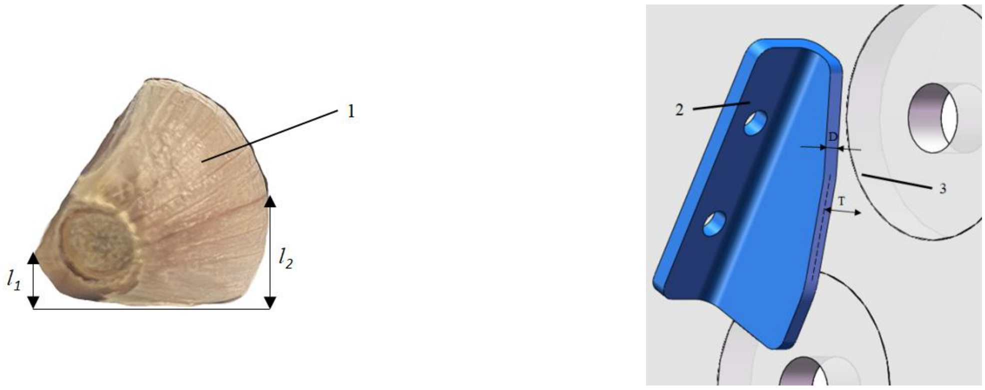

Fig. 4 - Garlic clove contact surface height
1 - Garlic clove; 2 - Guide cam; 3 - Seed plate.

Determination of tilt angle parameters

The determination of the inclination angle of the lead-in section (α_t) and the seeding section are crucial, as it directly influences the direction of the resultant force (F). If F points toward the center, it can cause the garlic clove to move radially, resulting in jamming and reduced sowing accuracy. To prevent this, the contact between the garlic clove and point *a* is analyzed. Ensuring point *a* does not cause jamming guarantees that as the clove contacts the *ab* section, the angle between the force and the suction hole center increases, thus avoiding jamming. By appropriately setting the α_t angle, λ_1 > 0 is maintained, ensuring smooth guidance of the garlic clove, as shown in Figure 5(a).

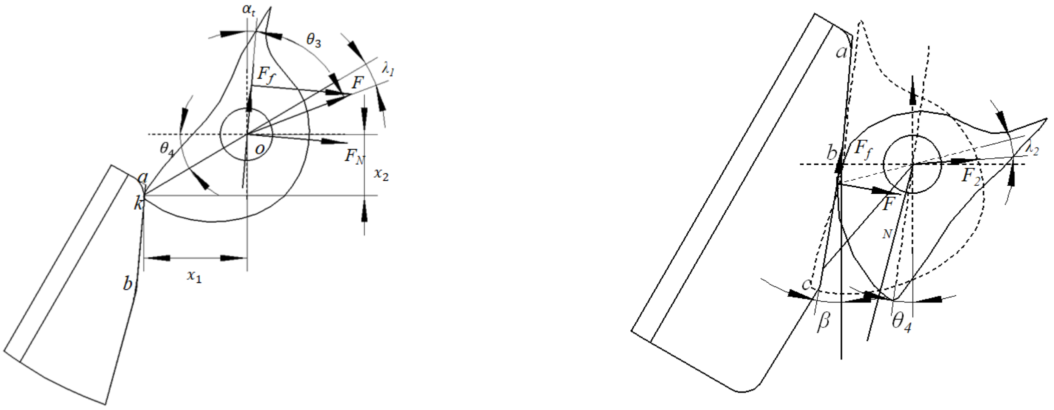

a) Analysis of the inclination angle of the lead-in section *b) Analysis of the tilt angle of the delivery section*

Fig. 5 - Garlic clove contact profile analysis

Geometric analysis of garlic clove contacting point a in the lead-in section:

$$\begin{cases} \tan\theta_4 = \dfrac{x_1}{x_2} \\ \theta_3 = \arccos\dfrac{F_f}{F_1} \\ \lambda_1 = \beta + \theta_4 + \theta_3 - 90^\circ \end{cases} \quad (8)$$

where: θ_4 - the angle between *ok* and the horizontal direction,°; λ_1 - the angle between *ok* and F, °;
x_1, x_2 - horizontal distance and vertical distance between k and O, mm.

Experimental measurements showed that for varying size ranges x_1 and x_2, $\theta_2 \approx 60°$, and θ_3 ranged from 20.5° - 25.6°. Substituting θ_2 and θ_3 into formula(13), when λ_1>0, the value range of α_t is 2.3° - 8.6°.

If $\beta < \alpha_t$, misguidance occurs ; if $\beta > \alpha_t$, root engagement fails, altering torque. β must position the force below the suction hole while ensuring root contact, as shown in Figure 5(b). For λ_2 > 0, β ranges from 10° to 30.3°. To avoid misdirection, β < 18.5°, setting the *bc* section's inclination between 13° and 19.5°.

Experimental materials and equipment

The *JPS-12* sowing bench test, with a modified air control system, positioned the negative pressure zone and seeding point 30° below the horizontal plane, as shown in Figure 7. Garlic cloves, categorized by thickness—A (12–15 mm, 30%), B (15–18 mm, 41%), and C (18–21 mm, 25%)—covered 96% of Jinxiang samples (*Li et al., 2022*). The guide cam and hopper are 3D printed using resin.

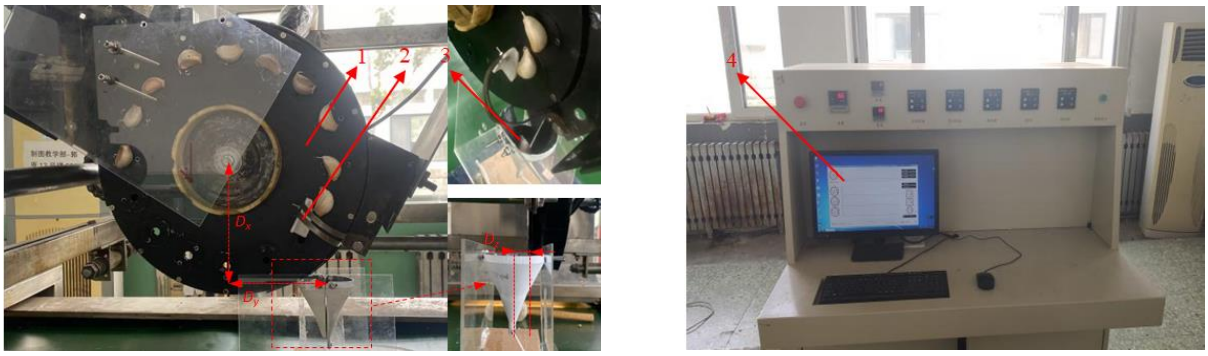

Fig. 7 – Bench testing of metering devices

1 - Metering device; 2 - Guide cam; 3 - Falling into the hopper in an upright position; 4 - Equipment Controls.

Test methods

(1) A five-factor, three-level design experiment was conducted in a stable environment with initial trials to determine α_t, β, D_X, D_Y and D_Z ranges. The optimal parameter combination was determined using the upright orientation rate (Y_1) as the evaluation index. The experimental structure code is shown in Table 1.

Table 1

Table of factors and levels

Level	Factors				
	Angle of the lead in section, α_t / °	Angle of the seeding section, β / °	Lateral distance, D_x / mm	Longitudinal distance, D_y / mm	Vertical distance, D_z / mm
-1	3	13	140	125	9
0	5	15	145	130	11
1	7	17	150	135	13

(2) Based on the experiment (1), a bench high-speed operation performance comparison test was conducted on the seed meter with and without additional guides. A two-factor experiment tested negative pressure across 10 gradients (-8.5 to -13 kPa) and rotational speed at 4 levels(6–9 rad/s).

The upright orientation rate(Y_1) evaluated the guide cam's effectiveness:

$$Y_1 = \frac{m_1}{Q} \times 100\% \tag{9}$$

where: m_1- the number of buds falling into the receiving hopper with the buds pointing upwards;

Q - total number of garlic cloves.

RESULTS

Analysis of test results

The results of the orthogonal test are shown in Table 2, where *A*, *B*, *C*, *D,* and *E* are structural coding values. Each group of tests was performed 4 times to obtain the average value.

Table 2

Experimental program and results

Number	Factors					Indicators	Number	Factors					Indicators
	A	*B*	*C*	*D*	*E*	Y_1		*A*	*B*	*C*	*D*	*E*	Y_1
1	-1	-1	0	0	0	92.6	24	0	1	1	0	0	95.8
2	1	-1	0	0	0	88.6	25	-1	0	0	-1	0	91.8
3	-1	1	0	0	0	94.5	26	1	0	0	-1	0	85.6
4	1	1	0	0	0	85.4	27	-1	0	0	1	0	88.8
5	0	0	-1	-1	0	93.8	28	1	0	0	1	0	82.4

Number	Factors					Indicators	Number	Factors					Indicators
	A	*B*	*C*	*D*	*E*	Y_1		*A*	*B*	*C*	*D*	*E*	Y_1
6	0	0	1	-1	0	94.6	29	0	0	-1	0	-1	93.6
7	0	0	-1	1	0	91.2	30	0	0	1	0	-1	94.2
8	0	0	1	1	0	90.2	31	0	0	-1	0	1	89.6
9	0	-1	0	0	-1	90.5	32	0	0	1	0	1	89.2
10	0	1	0	0	-1	93.4	33	-1	0	0	0	-1	88.6
11	0	-1	0	0	1	87.2	34	1	0	0	0	-1	84.5
12	0	1	0	0	1	82.6	35	-1	0	0	0	1	87.6
13	-1	0	-1	0	0	93.8	36	1	0	0	0	1	82.8
14	1	0	-1	0	0	86.1	37	0	-1	0	-1	0	92.6
15	-1	0	1	0	0	94.6	38	0	1	0	-1	0	93.8
16	1	0	1	0	0	86.8	39	0	-1	0	1	0	88.4
17	0	0	0	-1	-1	91.2	40	0	1	0	1	0	87.6
18	0	0	0	1	-1	92.4	41	0	0	0	0	0	95.6
19	0	0	0	-1	1	87.6	42	0	0	0	0	0	96.9
20	0	0	0	1	1	85.8	43	0	0	0	0	0	92.8
21	0	-1	-1	0	0	95.5	44	0	0	0	0	0	96.2
22	0	1	-1	0	0	92.6	45	0	0	0	0	0	97.4
23	0	-1	1	0	0	94.8	46	0	0	0	0	0	98.7

The test results were analyzed using Design-Expert software to establish a quadratic regression model for the upright orientation rate (Y_1). The model's significance was verified through Anova and regression coefficient tests, the results showed that the most significant factors were *A*, *D*, and *E*, Results are presented in Table 3. The responses between the important factors and their effects on Y_1 were analyzed by completing the response surface, as shown in Figure 8.

Table 3

Measured test data from variance analysis

Sources	Sum of Squares	Degrees of Freedom	Mean Square	F-value	P-value
Models	722.36	20	36.12	11.65	<0.0001 *
A	156.88	1	156.88	50.99	<0.0001 *
B	1.27	1	1.27	0.4082	0.5287
C	1.00	1	1.00	0.3225	0.5752
D	36.60	1	36.60	11.80	0.0021*
E	81.00	1	81.00	26.12	<0.0001 *
Lack of Fit	57.45	20	2.87	0.7154	0.7325
Pure Error	20.07	5	4.01	**R^2**	0.9131

*Note: * means extremely significant (P < 0.01)*

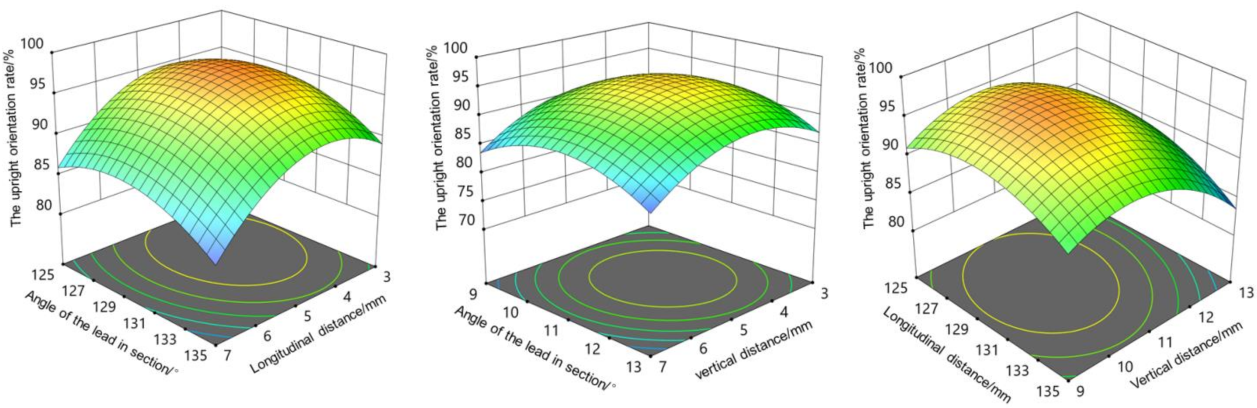

a) $E_C(A,D)$ *b) $E_C(A,E)$* *c) $E_C(D,E)$*

Fig. 8 – Bench testing of metering devices

Optimization of the model by parameter combination with Y_1 taking the maximum value of α_t=5°, β=15°, D_X=140mm, D_Y=128mm, D_Z=9mm. Verification tests with these parameters resulted in an average uprightness of 96.8%, which was determined to be the optimal parameter.

Comparative test

Table 4 compares the performance of devices *K* and *T* under varying pressures and speeds. Device *T*'s upright rate rose and then fell with increasing pressure; low pressure caused unstable C-size clove adsorption, while high pressure impeded posture adjustment. Optimal rates (>92%) were achieved at -10 to -12 kPa. Device *K*'s upright rate stabilized at -10 kPa after an initial rise.

Table 4

Comparison of the qualified index of *K* and *T* seeding devices (Short version)

Working speed (n) / (rad/s)	-8.5 kPa			-9 kPa			-9.5 kPa			-10 kPa			-10.5 kPa		
	K	T	Δ	K	T	Δ	K	T	Δ	K	T	Δ	K	T	Δ
6	66.3	67.2	-0.9	71.2	70.2	1.0	72.2	76.4	-4.2	78.5	82.6	-4.1	82.4	88.4	-6.0
7	63.2	61.2	-2	68.8	70.6	-1.8	75.8	78.0	-2.2	79.0	83.8	-4.8	84.2	90.2	-6.0
8	54.2	58.0	-3.8	63.4	60.4	3.0	60.2	61.8	-1.6	68.3	73.0	-4.7	76.3	84.6	-8.3
9	50.3	48.6	1.7	50.2	49.4	0.8	55.2	56.4	-1.2	68.0	70.4	-2.4	70.2	78.4	-8.2
Working speed (n) / (rad/s)	-11 kPa			-11.5 kPa			-12 kPa			-12.5 kPa			-13 kPa		
	K	T	Δ	K	T	Δ	K	T	Δ	K	T	Δ	K	T	Δ
6	82.6	93.4	-10.8	86.2	95.6	-9.4	82.0	94.6	-12.6	86.5	92.8	-6.3	82.0	89.6	-7.6
7	83.5	93.5	-10.0	87.6	98.8	-11.2	88.5	97.9	-9.4	87.6	94.4	-6.8	86.2	95.2	-9.0
8	83.5	90.8	-7.3	86.4	96.6	-10.2	83.4	94.2	-10.8	84.4	91.4	-7.0	81.3	90.6	-9.3
9	82.4	91.4	-9.0	85.6	95.8	-10.2	85.4	94.0	-9.6	84.6	92.6	-8.0	83.4	92.5	-9.1

Note: K represents the upright rate of the bud tip without a guide cam (%), T represents the upright rate with a guide cam (%), and Δ is the difference between the two rates (%)

As shown in Table 4, the difference in the vertical rate (Δ) highlights the guide cam's impact on seeders T and K. Δ increases and then decreases with pressure changes. At -8.5 to -10 kPa, ∣Δ∣ <5%, showing minimal impact. Between -10 and -12 kPa, Δ reaches up to 10%, significantly improving the vertical rate. At -11.5 kPa and 7 rad/s, the T seeder achieves a vertical rate of 98.8%, with Δ at -11.2%, confirming the guide cam's superior performance.

CONCLUSIONS

The traditional air-absorbing garlic clove metering device has been improved by adding a guiding cam to control the orientation of the garlic cloves so that the bud tips are discharged in an upward direction, which improves the stability of the sowing and meets the agronomic requirements. The analysis of garlic clove size and attitude determined the key parameters: introduction angle α_t = 5°, thickness D = 4 mm, and seeding section inclination β = 15°, D_X=140mm, D_Y=128mm, D_Z=9mm, enabling effective posture adjustment. Validation experiments showed the guide cam significantly improved upright rates. At -10.5kPa, the upright rate difference (Δ) exceeded 5%, reaching (Δ) to 10% at -11 to -12kPa. At -11.5kPa and 7 rad/s, the upright rate peaked at 97.2%, 11.2% higher than without the guide cam, confirming its design effectiveness.

ACKNOWLEDGEMENT

This research was supported by the Natural Science Foundation of Shandong Province (ZR2022ME103) and the 2022 Agricultural Application Technology Innovation Project of Jinan City (CX202216).

REFERENCES

[1] Babatunde S. (2020). Design and fabrication of an electrically powered maize planter. *Journal of Engineering Studies and Research*. Vol.26, pp. 204 -211.

[2] Chen C. (2016). *Structural design and performance test of belt-type seed guide device of precision seeder (精量播种机带式导种装置结构设计与性能试验研究)*, Master's thesis Inner, Mongolia Agricultural University.

[3] Chen Y., Han J., Lan Y., Zhang M., Jin Y., Zhang Z., Wang W. (2022). Design and experiment of the

combined seed guiding tube for precision metering device (精密排种器组合式导种管设计与试验). *Transactions of the Chinese Society of Agricultural Engineering*, Vol. 38, pp. 14-24.
[4] Dong J., Gao X., Zhang S., Huang Y., Zhang C., Shi J., (2023). Design and Test of Guiding Seed Throwing Mechanism for Maize Posture Control and Driving Metering Device (玉米姿控驱导式排种器导向投种机构设计与试验). *Transactions of the Chinese Society for Agricultural Machinery*, Vol.54, pp.25-34.
[5] Ji J., Sang Y., He Z., Jin X., Wang S. (2021). Designing an intelligent monitoring system for corn seeding by machine vision and Genetic algorithm-optimized back propagation algorithm under precision positioning. *Plos One*, Vol. 16, pp. 7-10.
[6] Kang J., Xiang Y., Zhang C., Peng Q., Zhang G. (2022). Analysis and experiments of the seed feeding performance of air-suction roller dibbler for peanuts (气吸滚筒式花生穴播器投种性能分析与试验). *Transactions of the Chinese Society of Agricultural Engineering (Transactions of the CSAE)*, Vol. 38, pp.1-11.
[7] Liao Y., Li C., Liao Q., Wang L., (2020). Research Progress of Seed Guiding Technology and Device of Planter (播种机导种技术与装置研究进展分析). *Transactions of the Chinese Society for Agricultural Machinery*, Vol. 51, pp. 1-14.
[8] Liu L., Yang H., (2015). 3D reverse engineering design on seed tube based on Geomagic Design software (基于 Geomagic Design 软件的导种管三维逆向工程设计). *Transactions of the Chinese Society of Agricultural Engineering*, Vol. 31, pp. 40-45.
[9] Liu S., Jia H., Wang J., (2022). Promotion and application of mechanization technology in garlic production (大蒜生产机械化技术的推广应用). *Promotion of Agricultural Machinery Technology*, Vol. 08, pp. 17-19.
[10] Liu Z., Xia J., Hu M., Du J., Luo C., Zheng K., (2021). Design and analysis of a performance monitoring system for a seed metering device based on pulse width recognition. *Plos One*, Vol. 16.
[11] Li C., (2022). Experimental study on garlic air-suction seed metering device for application of image recognition and orientation technology (便于图像识别定向技术应用的大蒜气吸式排种器的试验研究). Master's thesis Inner, Shandong University of Technology.
[12] Liu Q., (2017). *Design and experimental study of seed precision delivery mechanism of high-speed seeder (高速播种机种子精准投送机构设计与试验研究).* PhD dissertation, China Agricultural University.
[13] Ma C., Yi S, Tao G., Li Y., (2023). Mechanism Analysis and Parameter Optimization of Corn Seeds Receiving by Rotating Clamp of Belt-type Seed Guiding Device (带式玉米高速导种装置旋夹纳种机理分析与参数优化). *Transactions of the Chinese Society for Agricultural Machinery*, Vol.54, pp. 134-143.
[14] Wu X., Zhong Z., Tang L., (2024). Experimental study on the effects of different garlic planters and planting parameters on garlic planting efficiency (不同机型和播种参数对大蒜播种效果的影响). *Journal of Shenyang Agricultural University*, Vol. 55, pp. 474-482.
[15] Xu H., Li C., Feng R., Song J., Xiang H., (2021). Effect of garlic planting orientation on garlic growth and yield (蒜种种植方位对大蒜生长发育及产量的影响). *Journal of Chinese Agricultural University*, Vol.42, pp.74-78.
[16] Zhao S., Chen J., Wang J., Chen J., Yang C., Yang Y., (2018). Design and Experiment on V-groove Dialing Round Type Guiding-seed Device (精量播种机 V 型凹槽拨轮式导种部件设计与试验). *Transactions of the Chinese Society for Agricultural Machinery*, Vol. 49, pp. 146-158.